

N O T I C E

THIS DOCUMENT HAS BEEN REPRODUCED FROM
MICROFICHE. ALTHOUGH IT IS RECOGNIZED THAT
CERTAIN PORTIONS ARE ILLEGIBLE, IT IS BEING RELEASED
IN THE INTEREST OF MAKING AVAILABLE AS MUCH
INFORMATION AS POSSIBLE

(NASA-TM-81240) GLOBAL OPTIMALITY OF
EXTREMALS: AN EXAMPLE (NASA) 23 p
HC A02/ME A01

N81-13673

CSCL 12A

Unclass

G3/63 29486

Global Optimality of Extremals: An Example

Eliezer Kreindler and Frank Neuman

October 1980

NASA

National Aeronautics and
Space Administration

Global Optimality of Extremals: An Example

Eliezer Kreindler and
Frank Neuman, Ames Research Center, Moffett Field, California

NASA

National Aeronautics and
Space Administration

Ames Research Center
Moffett Field, California 94035

Global Optimality of Extremals: An Example

ELIEZER KREINDLER and FRANK NEUMAN

Abstract The question of the existence and the location of Darboux points (beyond which global optimality is lost) is crucial for minimal sufficient conditions for global optimality and for computation of optimal trajectories. Here, we numerically investigate the Darboux points and their relationship with conjugate points for a problem of minimum fuel, constant velocity, horizontal aircraft turns to capture a line. This simple second-order optimal control problem shows that ignoring the possible existence of Darboux points may play havoc with the computation of optimal trajectories.

E. Kreindler is a National Research Council Associate, Ames Research Center, NASA, Moffett Field, CA 94035, on leave from the Technion, Israel Institute of Technology, Haifa, Israel.

F. Neuman is with the Ames Research Center, NASA, Moffett Field, CA 94035.

1. Introduction

Optimal controls and optimal state trajectories are often investigated by computation of extremals, i.e., state trajectories satisfying the necessary conditions of the minimum principle. Thus, rather than solve a two-point-boundary-value problem, one integrates, for example, the state and costate differential equations from a given end state, with the end conditions on the costates as parameters. When the equations are integrated over a sufficiently long interval, local and global optimality of the extremals may unwittingly be lost, i.e., the integration crosses conjugate and Darboux points. (Conjugate and Darboux points are defined as time points on the time interval of interest, but usually also refer to the states on the extremal corresponding to these times.)

A point conjugate to an end point is one beyond which an extremal is no longer locally optimal hence its obvious importance; an early reference is [1], and a recent one is [2]. Yet, not all the results on conjugate points in the calculus of variations have been translated into the control context, particularly for bounded controls. The books by Hestenes [3] and Young [4], for instance, stop short of conjugate points in their discussion of optimal control theory. In practice, conjugate points are rarely tested for (however, see [5], [6], [7]); in fact, they are often simply ignored.

A Darboux point to an end point is one beyond which the extremal is no longer globally optimal [8]. A Darboux point often precedes a conjugate point, a fact apparently first recognized by Darboux [9], [10]; hence the name Darboux point assigned by Moyer and Kelly in [5]. There are no general tests for Darboux points, except for the case of quadratic performance integrals with nonlinear terminal terms, subject to linear differential equations and nonlinear end state constraints [11].

We encountered the vexing Darboux point phenomenon in our study of minimum fuel landing approach (to be published). Our objective here is to compute the extremals and to find the conjugate and Darboux points for a second-order special case to gain insight on their locations and their relationship.

II. The Example

We explore the question of Darboux points for a particular second-order example which derives from the problem of horizontal minimum-fuel aircraft turns to capture a line, such as would occur during a landing approach. To stay within the simplifying realm of two state variables we assume constant velocity and select the state variables x_1 and x_2 to represent the heading angle and the distance to the line, respectively; the control variable u represents the tangent of the bank angle. Under certain assumptions and suitable normalization the equations (see Appendix) are

$$\dot{x}_1 = -u, \quad x_1(t_f) = k2\pi, \quad k = 0, \pm 1, \dots, \quad (2.1)$$

$$\dot{x}_2 = \sin x_1, \quad x_2(t_f) = 0, \quad (2.2)$$

$$|u| \leq 1. \quad (2.3)$$

The cost integral is

$$J = \frac{2}{\pi(1+c)} \int_0^{t_f} (1 + cu^2) dt, \quad (2.4)$$

where t_f is free and c is a nonnegative constant (J is normalized with respect to the cost on an interval of length $\pi/2$, with $|u(t)| = 1$, i.e., the cost of a 90° turn at maximum bank angle).

We next compute families of all extremals by backward integration from the origin, $x(t_f) = (0, 0)$, plot curves of constant cost, and obtain loci of Darboux and conjugate points to the origin. The situation is complicated by the fact that states differing in the x_1 component by multiples of 2π are

equivalent states. Thus, on an extremal to the origin, there may be points beyond which the extremal is no longer globally optimal because nonneighboring extremals to $(k2\pi, 0)$ yield lower cost; we denote these points by $D_{k,2\pi}$, $k = 0, \pm 1, \dots$. According to the definition in [8], there can be only one Darboux point on an extremal: the first of the points $D_{k,2\pi}$ in the backward direction. We will call the other points pseudo-Darboux points. The concept of pseudo-Darboux point is applicable to other situations with a complicated set of end states.

Insight may be gained by referring to the aircraft turning problem (see Appendix). The aircraft trajectories in the horizontal plane are easy to draw because they are comprised of circular arcs when $|u| = 1$ and nearly straight lines when $|u| \rightarrow 0$ (as in Fig. 7). It should be noted, however, that the coordinates of the horizontal plane is not the state for this example; our analysis is in the $x_1 - x_2$ state plane for the problem stated in (2.1)-(2.4).

III. Computation of Extremals

The extremals are computed by application of the minimum principle [3].

The Hamiltonian H and costates λ_0 , λ_1 , and λ_2 are given by

$$H = \lambda_0(1 + cu^2) - \lambda_1 u + \lambda_2 \sin x_1, \quad (3.1)$$

$$\lambda_0 \geq 0, \quad \lambda_0 = \text{const}, \quad (3.2)$$

$$\dot{\lambda}_1 = -\lambda_2 \cos x_1, \quad (3.3)$$

$$\lambda_2 = \text{const}. \quad (3.4)$$

We consider extremals with $\lambda_0 \neq 0^*$; then, λ_0 can be set at $\lambda_0 = 1$.

*In the abnormal case, $\lambda_0 = 0$, we have $u = \text{sgn } \lambda_1$, $u \neq 0$, and $\lambda_1(t_f) = 0$. This yields only two extremals, which are identical to the extremals for $\lambda_0 = 1$ and $\lambda_2 = \pm c$.

Minimization of H with respect to u yields, for $c > 0$,

$$u = \begin{cases} 1, & \lambda_1 \geq 2c, \\ \lambda_1/2c & |\lambda_1| < 2c, \\ -1 & \lambda_1 \leq -2c. \end{cases} \quad (3.5)$$

Since t_f is unspecified, we have the condition

$$H|_{t_f} = 1 + cu^2(t_f) - \lambda_1(t_f)u(t_f) = 0. \quad (3.6)$$

Satisfying (3.5) and (3.6) yields

$$|u(t_f)| = \begin{cases} 1, & 0 < c \leq 1, \\ 1/\sqrt{c}, & c \geq 1, \end{cases} \quad (3.7)$$

and

$$\lambda_1(t_f) = \begin{cases} (1+c)\operatorname{sgn} u(t_f), & 0 < c \leq 1, \\ 2\sqrt{c} \operatorname{sgn} u(t_f), & c \geq 1. \end{cases} \quad (3.8)$$

It is evident from Eqs. (2.1), (2.2), (3.3), (3.5), and (3.8) that the extremals depend on two parameters: the sign of $u(t_f) \triangleq u_f$ and the value of the constant λ_1 . Thus, for a given c , we can group the extremals into four families:

$$\{u_f > 0, \lambda_1 \geq 0\}, \{u_f > 0, \lambda_1 < 0\}, \{u_f < 0, \lambda_1 \geq 0\}, \{u_f < 0, \lambda_1 < 0\}$$

Of these, it is easy to see that the third and fourth families are symmetrical about the origin to the first and second, respectively. The second family can also be obtained from the first (as comparison of Figs. 2 and 3 will reveal).

Figure 1 shows the first family of extremals together with curves of constant cost, $J = \text{const}$. The extremal for $\lambda_1 = -1.0$ asymptotically tends to the line $x_1 = \pi/2$. The extremals for $|\lambda_1| > 1$ are drawn only up to and slightly beyond the conjugate point, i.e., the contact with the envelope to

the family.[†] Since the remaining three families with their associated curves of constant cost can easily be obtained from the first, Fig. 1 can be transferred onto a transparent sheet to seek intersections of curves of constant cost of the first family with those of equal value of the other families [also of families of extremals to $(2k\pi, 0; k = \pm 1)$, no need to consider larger k 's]. In this example, these intersections determine the $D_{k2\pi}$ points.

Figure 2 shows the first family of extremals and the $D_{k2\pi}$ - loci, $k = 0, \pm 1$. The solid heavy curves are loci of Darboux points, the broken curve is the locus of pseudo-Darboux points, and the dash-dot curve is the locus of conjugate points. A few alternative equicost extremals from points on the $D_{k2\pi}$ - loci are shown. Consider, for instance, the extremal corresponding to $\lambda_2 = -1.1$, starting backwards from the origin. Beyond the point D_0 there exist lower cost extremals to the origin, of the fourth family; thus, D_0 is a Darboux point. Beyond the point $D_{-2\pi}$ there are lower cost extremals to $(-2\pi, 0)$, of the third family, but of higher cost than extremals of the fourth family to the origin. Thus, $D_{-2\pi}$ is a pseudo-Darboux point; the alternative equicost extremal from $D_{-2\pi}$ to $(-2\pi, 0)$ is shown. The contact point C with the envelope is a conjugate point to the origin beyond which the extremal in question is no longer locally optimal. Indeed, the cost from the point P , which is beyond the envelope contact for the $\lambda_2 = -1.1$ extremal, is $J_p(-1.1) = 4.61$, while for the neighboring $\lambda_2 = -1.04$ extremal it is $J_p(-1.04) = 4.57$. We note that from the state $(-\pi, 0)$, the intersection of the D_0 - locus and the $D_{-2\pi}$ - locus, there are four globally optimal

[†]We assume that the envelope theorem of the calculus of variations (e.g., [4]) holds here; then the envelope contact points are conjugate points. At any rate, the subsequent discussion shows numerically that local optimality is lost past the contact points.

extremals; two to the origin and two to $(-2\pi, 0)$. We also note that the Darboux and conjugate points coincide only on the abnormal extremal, $\lambda_2 \rightarrow \infty$ (see footnote on p. 4). (For interpretation of Darboux points in terms of the aircraft trajectories in the horizontal plane, see Fig. 7 where the x_3 - axis is the line to be captured.)

Figure 3 shows the second family of extremals with details as in Fig. 2. Note that all the extremals coincide on the arc from $(\pi, -2)$ to the origin (representing a final 180° turn at maximum bank angle). For $\lambda_2 \geq 1.04$, the Darboux points are on the D_0 - locus, (the segment $\{x: x_1 = \pi, -2 \leq x_2 \leq 0\}$), while for $\lambda_2 < 1.04$ the Darboux points are on the $D_{2\pi}$ - locus. The extremals of this family are globally optimal only for initial states restricted to the shaded area shown in the figure.

Having obtained the loci of the Darboux points, we can determine a strip of width 2π in the state plane with all globally optimal trajectories to the origin, as shown in Fig. 4. The strip is symmetrical about the origin. Initial states outside this strip have globally optimal trajectories to $(k2\pi, 0)$, $k = \pm 1, \dots$; however, they can be shifted by a multiple of 2π to an equivalent initial state inside the strip. The globally optimal trajectories are unique, except those from initial states on the segments $\{x: x_1 = \pi, -2 < x_2 \leq 0\}$, and $\{x: x_1 = -\pi, 0 \leq x_2 < 2\}$. All optimal trajectories starting at initial states with $x_2 \leq 0$ end with $u_f = 1$, except those in the vertically shaded area which end with $u_f = -1$. The optimal control is mostly $|u(t)| \leq 1$, except in the horizontally shaded areas where $|u(t)| < 1$.

Results are shown only for $c = 0.1$ (which corresponds to the fuel flow characteristics of a jet transport at sea level); the cases $c = 1$ and $c = 10$ were examined and seen to be qualitatively similar. We also examined

the case $c = 0$, the time optimal case, previously treated from a different perspective by Erzberger and Lee [12]. The resulting families of extremals and $D_{k2\pi}$ - loci are quite similar to those for $c > 0$, but with corners and straight lines (caused by u switching between the values $\pm 1, 0$).

IV. Conclusions

It is the crucial importance of Darboux points in computing globally optimal trajectories and the scarcity of results that motivated us to report in detail on a particular problem. We find that on some extremals the Darboux point is a D_0 point (e.g., on the extremal $\lambda_2 = -1.3$ in Fig. 2) while on others the Darboux point is a $D_{-2\pi}$ point (e.g., $\lambda_2 = -1.0001$ in Fig. 2) or a $D_{2\pi}$ point (e.g., $\lambda_2 = -0.999$ in Fig. 2). We observe in Figs. 2 and 3 that only the Darboux points on the extremals for $|\lambda_2| > 1$, where u does change sign, are followed by conjugate points. Therefore, it does not appear profitable in this example to search for the Darboux points by testing for conjugate points. Also, on most extremals the conjugate point is far behind the Darboux point. For example, for the extremal for $\lambda_2 = 1.3$ in Fig. 3, backwards from the origin, the conjugate point C occurs about 80% later than in the Darboux point D_0 .

As illustrated here, the question of the existence of Darboux points cannot be lightly dismissed nor easily answered. We hope to have stimulated an awareness of the problem and of the need for further research.

Appendix: Derivation of Eqs. (2.1)-(2.4)

The airplane is flying at constant velocity v in the horizontal $x - y$ plane, with the heading angle ψ as shown in Fig. 5. Figure 6 shows the lift force L , the weight W and the bank angle ϕ which is constrained by

$$|\phi| \leq \phi_{\max} . \quad (A1)$$

Neglecting the vertical component of the thrust T , we have the constraint

$$L \cos \phi = W . \quad (A2)$$

Assuming constant mass m , we have

$$mv \frac{d\psi}{dt} = -L \sin \phi = -\frac{W \sin \phi}{\cos \phi} = -mg \tan \phi .$$

The equations of motion are therefore

$$\begin{aligned} \frac{d\psi}{dt} &= -\frac{g}{v} \tan \phi , \\ \frac{dy}{dt} &= v \sin \psi , \\ \frac{dx}{dt} &= v \cos \psi . \end{aligned} \quad (A3)$$

We use the nondimensional time

$$\tau = tv/R , \quad (A4)$$

where R is the (smallest) radius of turn for $|\phi| = \phi_{\max}$,

$$R = \frac{v}{|\dot{\psi}_{\max}|} = \frac{v^2}{g \tan \phi_{\max}} . \quad (A5)$$

Then (A3) becomes

$$\left. \begin{aligned} \dot{x}_1 &= -u , \\ \dot{x}_2 &= \sin x_1 , \\ \dot{x}_3 &= \cos x_1 , \end{aligned} \right\} \quad (A6)$$

where

$$x_1 = \psi , \quad x_2 = y/R , \quad x_3 = x/R , \quad u = \tan \phi / \tan \phi_{\max} , \quad (A7)$$

and the dot represents $d/d\tau$. Hence Eqs. (2.1)-(2.3), where we denote the nondimensional time by t .

We assume that the fuel flow depends on the thrust according to

$$\text{Fuel Flow} = c_0 + c_1 T . \quad (\text{A8})$$

Assuming zero sideslip, constant velocity requires that thrust equal drag.

The drag is assumed to be given by

$$D = k_1 v^2 + \eta L \alpha ,$$

where k_1 and η are constants and α is the angle of attack. Assuming further that

$$L = kv^2 \alpha ,$$

where k is a constant, we have, using (A2),

$$D = k_1 v^2 + \frac{\eta k v^2}{kv^2 \cos^2 \phi} = k_1 v^2 + \frac{k_2}{v^2} (1 + \tan^2 \phi) .$$

The fuel consumption is therefore given by

$$\text{Fuel Consumption} = \int_0^{t_f} [(c_0 + c_1 k_1 v^2 + c_1 k_2 / v^2) + (c_1 k_2 / v^2) \tan^2 \phi] dt ,$$

where the terms in parentheses are constants. Hence the performance integral for minimum fuel is of the form given in Eq. (2.4).

In the optimal control problem of capturing the line $y = 0$ with $\psi(t_f) = 0$, the state variable $x_3 = x/R$ in (A6) can be ignored; it is required, of course, for the flight trajectories in the horizontal plane. The plot of such trajectories is useful for the interpretation of Darboux points as shown in Fig. 7 which illustrates $D_{-2\pi}$ and D_0 Darboux points. In the backward direction, the heavy-line trajectories are globally optimal up to and including the points $D_{-2\pi}$ and D_0 . From the points $D_{-2\pi}$ and D_0 there exist equicost alternative trajectories, while beyond these points there exist lower cost trajectories, e.g., those shown in dashed curves from

the points A. On the other hand, the conjugate points are not usefully interpreted by horizontal flight trajectories.

References

- [1] J. V. Breakwell and Y. C. Ho, "On the conjugate point condition for the control problem," Int. J. Eng. Sci., vol. 2, pp. 565-570, 1965.
- [2] P. M. Mereau and W. F. Powers, "Conjugate point properties for linear quadratic problems," J. Math. Anal. Appl., vol. 55, pp. 418-433, 1976.
- [3] M. R. Hestenes, Calculus of Variations and Optimal Control Theory, New York: John Wiley & Sons, Inc., 1966.
- [4] L. C. Young, Lectures on the Calculus of Variations and Optimal Control Theory, Philadelphia, PA: Saunders, 1969.
- [5] H. G. Moyer and H. J. Kelley, "Conjugate Points on Extremal Rocket Paths," Proc. of the 19th Int. Astronautical Congress, New York, 1968, vol. 2, pp. 163-172. Pergamon Press, London, 1970.
- [6] H. G. Moyer, "A computer survey of impulsive ellipse-ellipse transfer," AIAA J., vol. 9, no. 2, pp. 321-323, 1971.
- [7] H. G. Moyer, "Optimal control problems that test for envelope contacts," JOTA, vol. 6, no. 4, pp. 287-298, 1970.
- [8] P. M. Mereau and W. F. Powers, "The Darboux point," JOTA, vol. 17, nos. 5/6, pp. 545-559, 1975.
- [9] O. Bolza, Vorlesungen über Variationsrechnung, p. 438, Teubner, Leipzig, 1909, reprinted by Chelsea Publ. Co., New York, 1963.
- [10] G. Darboux, Sur la Theorie des Surfaces, vol. III, p. 89, Gauthiers-Villars, Paris, 1894.
- [11] P. M. Mereau and W. F. Powers, "Characterization of the Darboux point for particular classes of problems," JOTA, vol. 22, no. 4, pp. 537-562, 1977.
- [12] H. Erzberger and H. Q. Lee, "Optimum horizontal guidance techniques for aircraft," J. Aircraft, vol. 8, no. 2, pp. 95-101, 1971.

Figure Captions

Fig. 1. Extremals and curves of constant cost for the family

$$\{u_f = 1, \lambda_2 < 0\}, c = 0.1.$$

Fig. 2. Family $\{u_f = 1, \lambda_2 < 0\}$, $c = 0.1$, loci of D-points, and alternative equicost extremals.

Fig. 3. Family $\{u_f = 1, \lambda_2 > 0\}$, $c = 0.1$, loci of D-points, and an alternative equicost extremal.

Fig. 4. Strip of width 2π with globally optimal trajectories to origin.

Fig. 5. Top view of aircraft in $x - y$ plane.

Fig. 6. Rear view of aircraft.

Fig. 7. Illustration of Darboux points in the horizontal plane.

(a) A $D_{-2\pi}$ Darboux point. (b) A D_0 Darboux point.

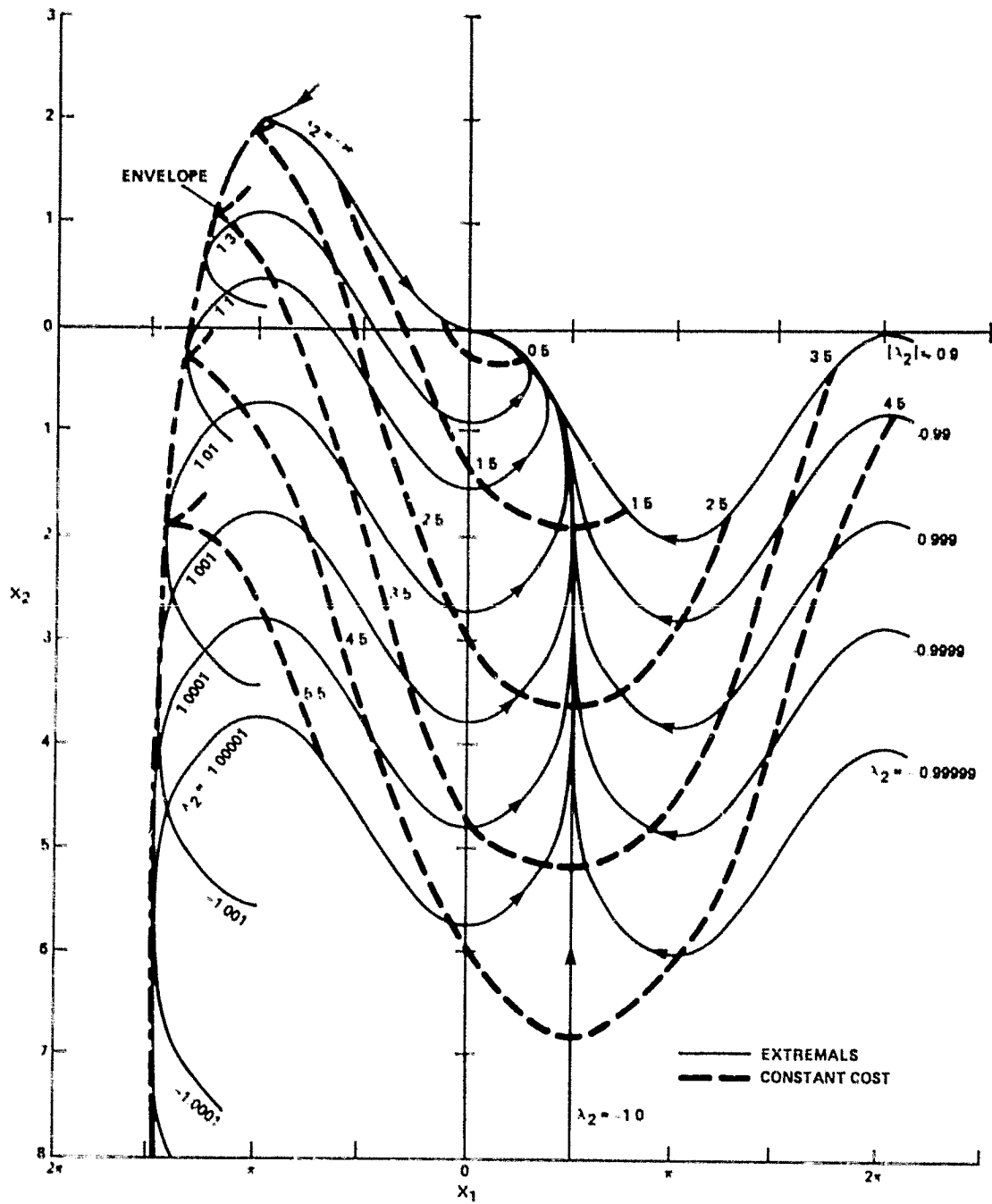


Fig. 1

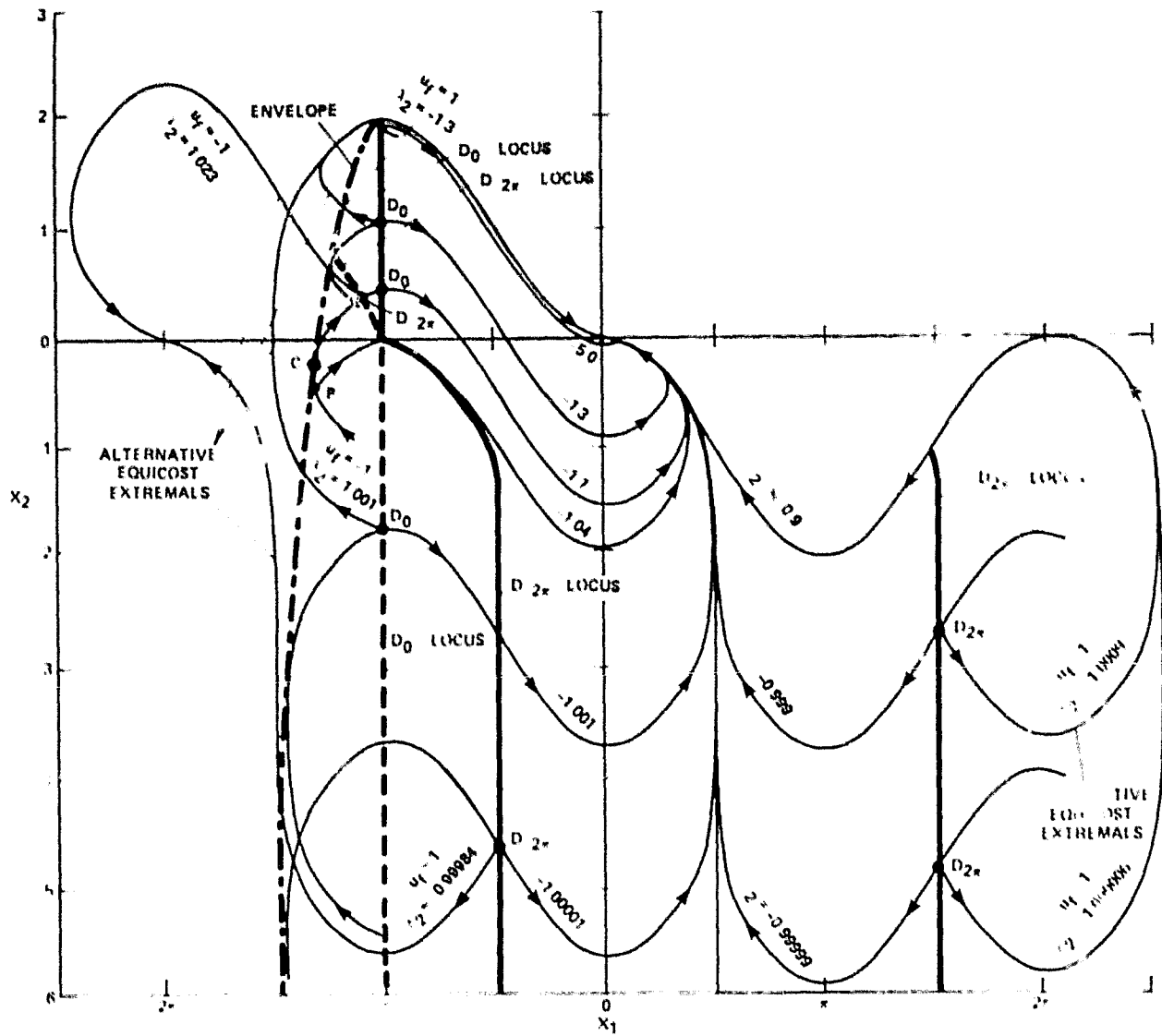


Fig. 2

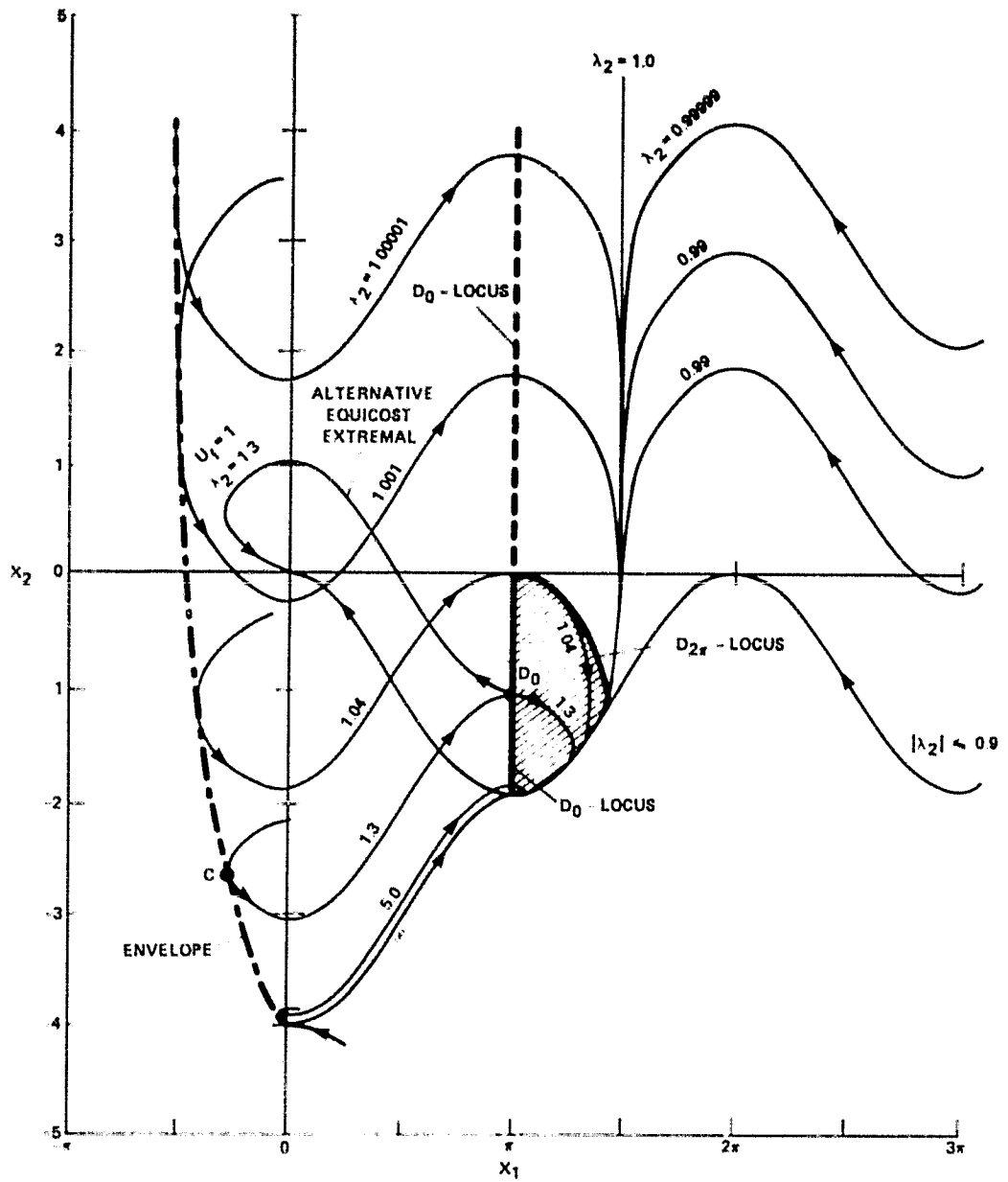


Fig. 3

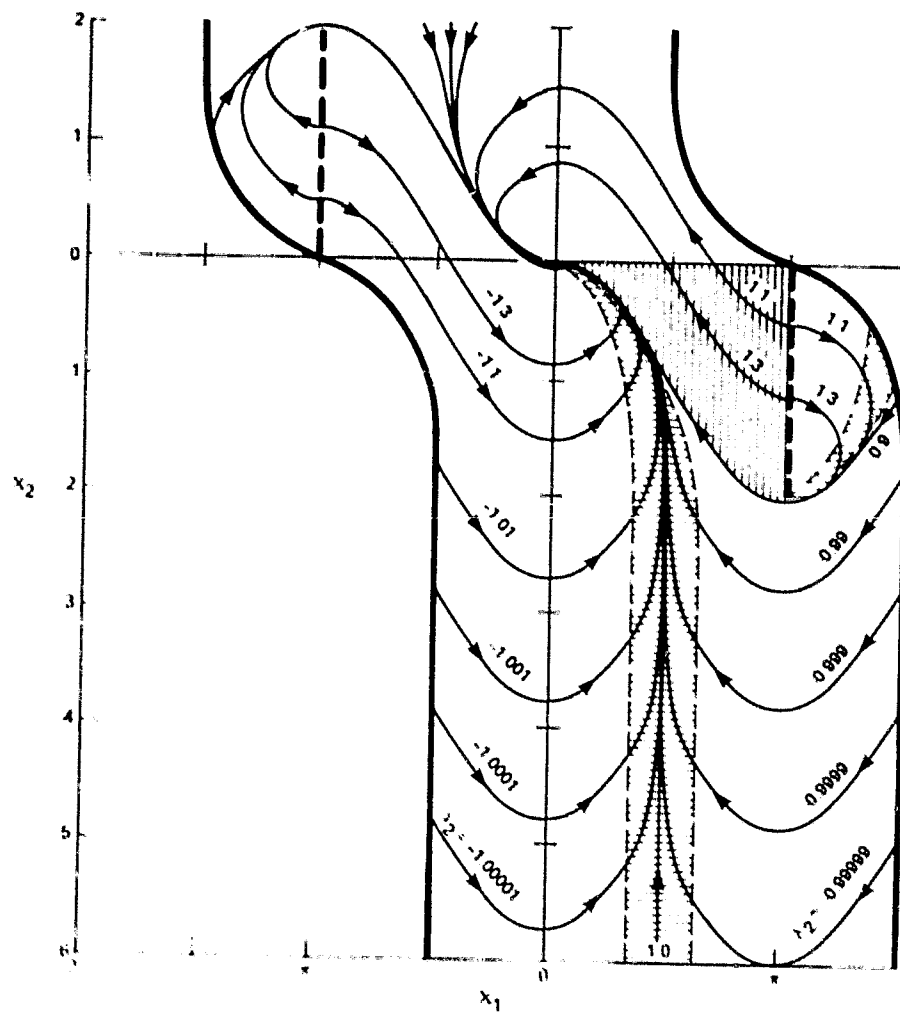


Fig. 4

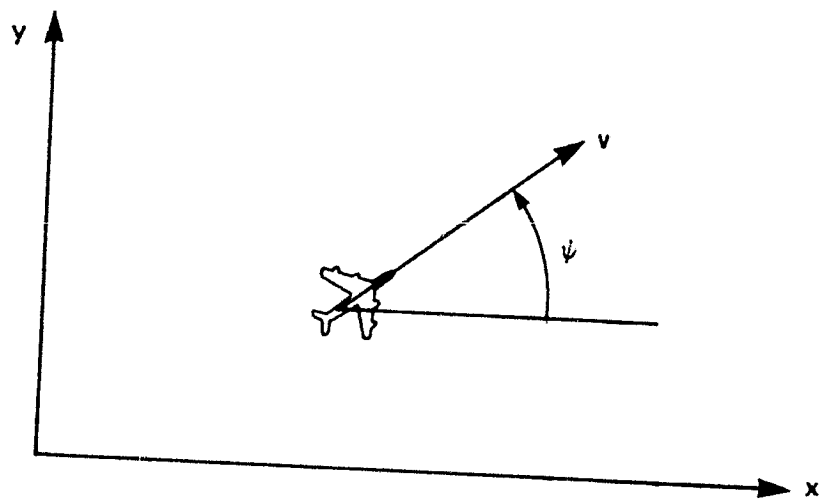


Fig. 5

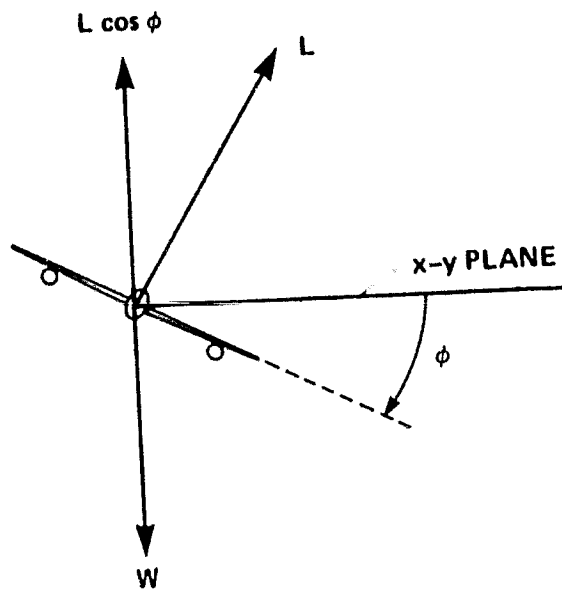


Fig. 6

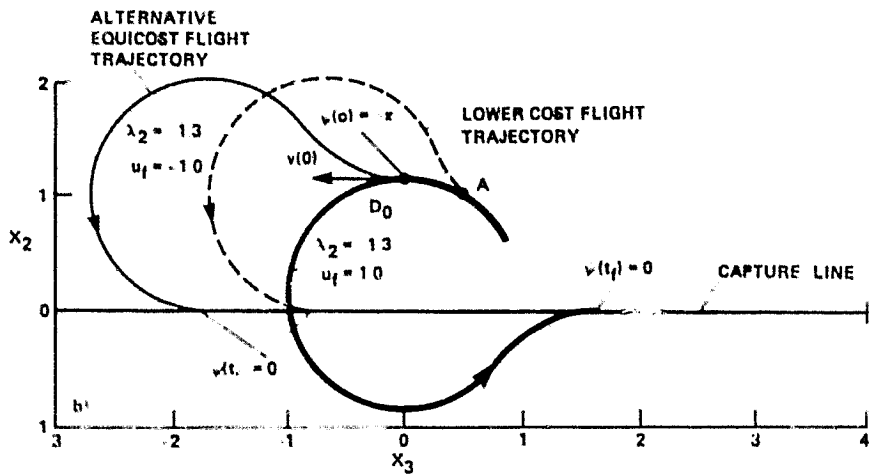
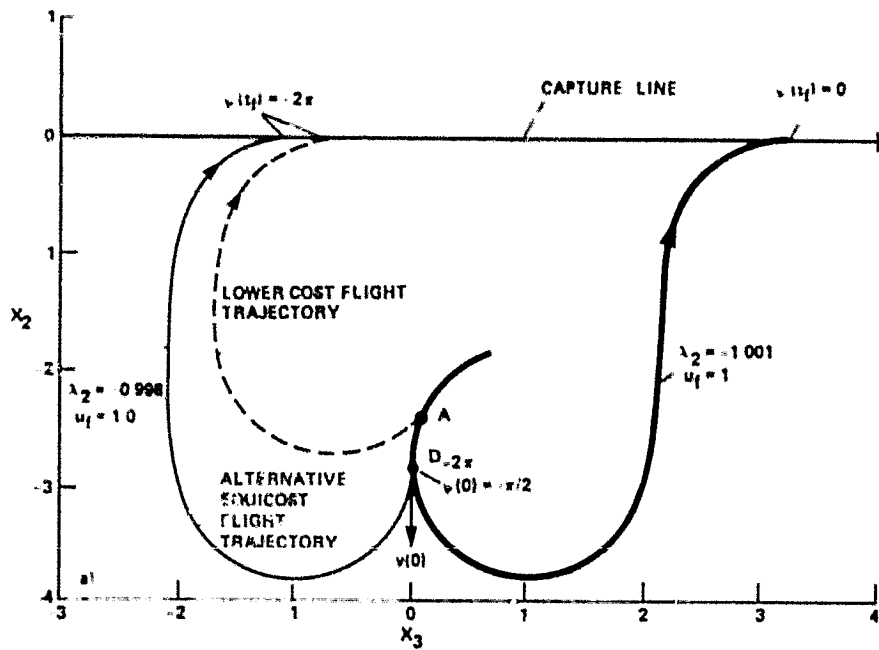


Fig. 7